Robust MPC with Support Vector Clustering-based Parametric Uncertainty Set for Building Thermal Control

Naharudinsyah, Ilham; Delfos, Rene; Keviczky, Tamas

DOI
10.1016/j.ifacol.2024.09.025

Publication date
2024

Document Version
Final published version

Published in
IFAC-PapersOnline

Available online at www.sciencedirect.com

ScienceDirect

IFAC PapersOnLine 58-18 (2024) 159–164

Robust MPC with Support Vector Clustering-based Parametric Uncertainty Set for Building Thermal Control*

Ilham Naharudinsyah * **Rene Delfos** ** **Tamas Keviczky** ***

* *Process and Energy Department, Faculty of Mechanical Engineering, Delft University of Technology, Delft, 2628 CN Netherlands (e-mail: I.Naharudinsyah@tudelft.nl).*

** *Process and Energy Department, Faculty of Mechanical Engineering, Delft University of Technology, Delft, 2628 CN, Netherlands (e-mail: R.Delfos@tudelft.nl).*

*** *Delft Center of Systems and Control, Faculty of Mechanical Engineering, Delft University of Technology, Delft, 2628 CD, Netherlands (e-mail: T.Keviczky@tudelft.nl).*

Abstract: Control systems are essential to support the use of building structures as short-term thermal energy storage (TES). Due to modeling and forecast imperfections, the controller must be able to deal with uncertainties. This paper proposes a robust model predictive controller (MPC) with a new uncertainty set construction technique to regulate the heat supply in a building envelope. We extend the Support Vector Clustering-based set construction technique to estimate modeling and forecast uncertainty sets. Subsequently, we integrate the sets into a Min-Max MPC framework to ensure robust feasibility by tightening the constraints. The resulting controller successfully deals with modeling and forecast uncertainties. The quality of the presented framework is compared with a nominal MPC and a robust MPC with different uncertainty set estimates. On the basis of a numerical simulation, we demonstrate that the proposed controller successfully maintains the room temperature within the comfort limits. The result also shows that our MPC is less conservative than the controller designed using a box-shaped non-falsified parametric uncertainty set.

Keywords: Support vector clustering, Set-membership estimation, Parametric uncertainty, Robust model predictive control, Thermal energy storage, Building energy systems

1. INTRODUCTION

Buildings represent a potential source of thermal energy flexibility in district heating systems (Verbeke and Audenaert, 2018). Due to their thermal inertia, they can be used to store heat energy for a short time. This can be done by providing an excessive amount of heat during times of excessive availability and allowing the building to release heat during the peak load or shortage period. When this mechanism is carried out, it is necessary to ensure the thermal comfort of the occupants. In order to avoid violation of thermal comfort, a building model is often required. Unfortunately, this model is not available to energy suppliers who wish to exploit the thermal inertia of a building. Therefore, in most cases, an approximate model is used.

An approximate building model can be obtained using a first-principles or a data-driven approach (Reynders et al., 2014). Data-driven modeling techniques, such as system identification, enable us to merge mathematical models and historical datasets to derive a temperature evolution model of a building. By using this approach, the time-consuming measurement of numerous parameters of building components can be avoided.

Despite its efficacy, the resulting model suffers from parametric uncertainties. Such errors often compromise the performance of the controller. Extensive research has been conducted to estimate parametric uncertainties. One of the notable techniques is set-membership estimation (Milanese and Vicino, 1991). By using this technique, a convex set that contains the true uncertainty value is constructed from historical data points. This method can be combined with MPC to minimize the energy use of buildings while ensuring the satisfaction of the operational constraints. Although the resulting uncertainty set can contain the true uncertainty value, the resulting uncertainty sets can be overly conservative. Such a set may lead to higher energy consumption to guarantee constraint satisfaction.

For additive uncertainty, Shang et al. (2017) developed an uncertainty set estimation strategy. This strategy successfully creates a polyhedral set that encloses the historical uncertainty data points with minimal volume. The uncertainty set is developed using the support vector clustering (SVC) method (Ben-Hur et al., 2001). The resulting set has a minimum distance with respect to its support vec-

* This work is supported by the WarmingUP project grant from the Netherlands Enterprise Agency (RVO).

10.1016/j.ifacol.2024.09.025

tors. Unfortunately, the technique cannot be implemented directly to construct a parametric uncertainty set because the parametric uncertainty data is not directly available to be used for the learning process.

In this work, we propose a new set-membership-based robust model predictive control strategy. We extend the kernel-learning-based set construction method proposed by Shang et al. Our strategy addresses the limitation of the existing approaches in constructing parametric uncertainty set by reformulating a SVC set to be used as a non-falsifying set. The non-falsified sets is used to refine the parametric uncertainty set estimate. Subsequently, we design an min-max MPC with the parametric uncertainty set estimate. Using numerical simulations, we show that the controller successfully schedules the heat supply to a building while ensuring that the temperature trajectory stays within the comfort bounds. The controller is also less conservative compared to another robust MPC formulation that uses a box uncertainty set as the non-falsifying set for the parametric uncertainty set construction.

The remainder of this article is structured as follows. In Section 2, we present the building model, the set membership estimation process, and the formulation of the optimal control problem. Section 3 details the setup of the numerical simulation. In Section 4, we discuss the simulation results. We conclude our work in Section 5.

2. METHODOLOGY

2.1 Building Model

In this work, we consider a residential building as an example. The mathematical model of a building can be derived using the building heat balance equation (Pothof et al., 2023). In this study, we employed the gray-box modeling technique. We modeled a building using the 2R2C model, where the parameters of the state-space matrices are obtained using system identification. This dynamical model has two states, namely room temperature T_z and lumped envelope temperature T_e. The input of this system is the heat energy Φ_h. In this system, the ambient temperature T_a and the solar radiation Φ_s are treated as disturbances.

The continuous-time state-space equation that represents the building is

$$\dot{x}(t) = A_c(w_\theta)x(t) + B_{d,c}(w_\theta)d(t) + B_{u,c}(w_\theta)u(t), \quad (1a)$$
$$y(t) = C_c x(t). \quad (1b)$$

The state-space matrices in (1) are given by:

$$A_c(w_\theta) = \begin{bmatrix} -\theta_1^* - w_{\theta_1} - \theta_2^* - w_{\theta_2} & \theta_2^* + w_{\theta_2} \\ \theta_3^* + w_{\theta_3} & -\theta_3^* - w_{\theta_3} \end{bmatrix}, \quad (2a)$$

$$B_{d,c}(w_\theta) = \begin{bmatrix} (\theta_1^* + w_{\theta_1}) & (\theta_4^* + w_{\theta_4}) \\ 0 & 0 \end{bmatrix}, \quad (2b)$$

$$B_{u,c}(w_\theta) = \begin{bmatrix} \theta_4^* + w_{\theta_4} \\ 0 \end{bmatrix}, \quad (2c)$$

$$C_c = [0 \ 1], \quad (2d)$$

where $x = [T_z,\, T_e]^\top \in \mathbb{R}^2$ is the state vector, $u = \Phi_h \in \mathbb{R}$ is the control input, and $d = [T_a,\, \Phi_s]^\top \in \mathbb{R}^2$ is an uncertain disturbance. In addition to the disturbance, the dynamical model also suffers from building modeling uncertainty $w_\theta = [w_{\theta_1},\, w_{\theta_2},\, w_{\theta_3},\, w_{\theta_4}]^\top \in \mathbb{R}^4$ due to parameter estimation process. The parametric uncertainty represents a constant but unknown error in the model parameters. Here, the parameter vector $\theta^* = [\theta_1^*,\, \theta_2^*,\, \theta_3^*,\, \theta_4^*]^\top \in \mathbb{R}^4$ is the true unknown value defined as follows:

$$\theta_1 = \frac{1}{R_z C_z}, \quad \theta_2 = \frac{1}{R_e C_z}, \quad \theta_3 = \frac{1}{R_e C_e}, \quad \theta_4 = \frac{1}{C_z}.$$

R_e and R_z denote the thermal resistance between the building and outside air, and between the inside air and the building envelope, respectively. C_e and C_z represent the thermal capacity of the building envelope and the thermal capacity of the air within the building, respectively.

The state-space equation is discretized with the sampling period T_s. The discrete-time state-space model is given by

$$\begin{aligned} x_{k+1} &= A(w_\theta)x_k + B_u(w_\theta)u_k + B_d(w_\theta)d_k, \\ y_k &= Cx_k, \end{aligned} \quad (3)$$

where the relations between continuous-time and discrete-time state-space matrices are as follows

$$A(w_\theta) = I_2 + A_c(w_\theta)T_s, \quad (4a)$$
$$B_d(w_\theta) = B_{d,c}(w_\theta)T_s, \quad (4b)$$
$$B_u(w_\theta) = B_{u,c}(w_\theta)T_s, \quad (4c)$$
$$C = C_c. \quad (4d)$$

Here, $I_2 \in \mathbb{R}^{2\times 2}$ denotes an identity matrix.

2.2 Parametric Uncertainty Estimation

The system matrices A, B_u, and B_d can be written as an affine function of uncertainties as follows:

$$[A(w_\theta) \ B_\mathrm{u}(w_\theta) \ B_\mathrm{d}(w_\theta)] = \left[\bar{A} \ \bar{B}_u \ \bar{B}_d\right] + \sum_{i=1}^{4} [A_i \ B_{d,i} \ B_{u,i}]\, w_{\theta_i}. \quad (5)$$

Here, $\bar{A} = A(0)$, $\bar{B}_\mathrm{u} = B_\mathrm{u}(0)$, and $\bar{B}_u = B_u(0)$ are state-space matrices with the unknown true parameter values, whereas $\{A_i,\, B_{d,i},\, B_{u,i}\}_{i=1}^4$ are known matrices, obtained, for instance, from a gray-box system identification process. The parametric uncertainty w_θ is assumed to lie inside a known, bounded, and convex set as follows

$$\mathcal{W}_{\theta,0} = \{w_\theta \,|\, H_\mathrm{w} w_\theta \leq h_\mathrm{w}\}. \quad (6)$$

A set estimation procedure is applied to refine the initial uncertainty set so that at each time step, the parametric uncertainty set is updated. The updated set satisfies

$$\mathcal{W}_{\theta,k+1} \subset \mathcal{W}_{\theta,k} \cap \Delta_k. \quad (7)$$

In this paper, the Support Vector Clustering (SVC) technique (Shang et al., 2017) is used to determine the non-falsified set Δ_k. The non-falsified set Δ_k is given by

$$\begin{aligned} \Delta_k = \{w_\theta : \, w_k = x_{k+1} - A(w_\theta)x_k - B_d(w_\theta)d_k \\ - B_u(w_\theta)u_k \in \mathcal{W}_s\} = \{w_\theta : \, H_w w_\theta \leq h_w\}. \end{aligned} \quad (8)$$

The additive uncertainty w_k is assumed to be in an unknown, convex, bounded polytope. The SVC technique is applied to obtain a tight polytope. In this technique, we use a data set $D = \left\{w^{(i)},\, d^{(i)},\, u^{(i)}\right\}_{i=0}^{N_D}$ consisting of historical additive uncertainties, past disturbances, and past control inputs, to construct a polytope that contains the parametric uncertainty in the following form:

$$\mathcal{W}_s = \left\{ w \;\middle|\; \begin{array}{c} \exists p_i,\ i,j \in \mathbb{N}_1^{N_D} \quad \text{s.t.} \sum_{i\in \text{SV}} \alpha_i \mathbf{1}_{n_x}^T p_i \leq \theta, \\ -p_i \leq Q\left(w^{(i)} - w^{(j)}\right) \leq p_i \end{array} \right\}, \tag{9}$$

where

$$\theta = \sum_{i\in\mathcal{I}_s} \alpha_i \left\| Q\left(w^{(s)} - w^{(i)}\right)\right\|_1,\ s \in \mathcal{I}_b. \tag{10}$$

Here, Q denotes a whitening matrix (Kessy et al., 2018). This matrix is applied to eliminate the cross-correlation such that the dimension of the transformed data similarly affects the kernel expression (Shang et al., 2017). p_i is an auxillary parameter that is used to reformulate the original form of the uncertainty set into a polytope (Shang et al., 2017). $\mathbf{1}_n$ denotes 1-vector of size n. The set $\mathcal{I}_s$ and $\mathcal{I}_b$ contain the indices of the data points that act as support vectors (SV) and boundary support vectors (BSV), respectively. α_i denotes the Lagrange multipliers for each of the data points. α_i, $\mathcal{I}_s$, and $\mathcal{I}_b$ can be obtained by applying the SVC algorithm to the data set D. In order to obtain a set in the form of (9), we employ the weighted generalized intersection kernel (WGIK) (Shang et al., 2017). Due to the polytopic structure of $\mathcal{W}_s$, it is convenient to formulate a tractable robust optimization problem using an SVC-based uncertainty set.

To construct a non-falsified parameter set based on SVC, we need to determine the relation between H_w, h_w, and w_k. For the sake of brevity, the additive uncertainty is expressed as follows:

$$x_{k+1} = \bar{A}x_k + \bar{B}_u u_k + \bar{B}_d d_k + \phi(x_k, d_k, u_k) w_\theta, \tag{11}$$

where

$$\phi_k = \phi(x_k, d_k, u_k) = [A_1 x_k + B_{u,1} u_k \ \cdots \ A_4 x_k + B_{u,4} u_k]. \tag{12}$$

In the subsequent parts of this paper, we refer to $\phi_k w_\theta$ as *parametric uncertainty-induced additive uncertainty*. As a first step in formulating the non-falsified parameter set, we substitute the additive uncertainty w_k into (9). The inequalities are divided into two parts as follows:

$$Qe_k - Q\phi_k w_\theta - Qw^{(i)} \leq p_i,\ \forall i \in N_D, \tag{13a}$$

$$-Qe_k + Q\phi_k w_\theta + Qw^{(i)} \leq p_i,\ \forall i \in N_D. \tag{13b}$$

where

$$e_k = x_{k+1} - (\bar{A}x_k + \bar{B}_d d_k + \bar{B}_u u_k). \tag{14}$$

By rearranging the inequalities (13) and multiplying them by $1_{n_x}^\top$, we obtain the following expression:

$$-\mathbf{1}_{n_x}^\top Q\phi_k w_\theta \leq \mathbf{1}_{n_x}^\top \left(p_i + Qw^{(i)} - Qe_k\right), \forall i \in N_D, \tag{15a}$$

$$\mathbf{1}_{n_x}^\top Q\phi_k w_\theta \leq \mathbf{1}_{n_x}^\top \left(p_i - Qw^{(i)} + Qe_k\right), \forall i \in N_D. \tag{15b}$$

By stacking all inequalities, (15) can be reformulated as follows:

$$-\mathbf{1}_{N_d} \otimes (\mathbf{1}_{n_x}^\top Q\phi_k) w_\theta \leq \begin{bmatrix} \mathbf{1}_{n_x}^\top p_1 \\ \vdots \\ \mathbf{1}_{n_x}^\top p_{N_D} \end{bmatrix} + \begin{bmatrix} \mathbf{1}_{n_x}^\top Qw^{(1)} \\ \vdots \\ \mathbf{1}_{n_x}^\top Qw^{(N_D)} \end{bmatrix} - \mathbf{1}_{N_D} \otimes \left(\mathbf{1}_{n_x}^\top Qe_k\right) \tag{16a}$$

$$\mathbf{1}_{N_d} \otimes (\mathbf{1}_{n_x}^\top Q\phi_k) w_\theta \leq \begin{bmatrix} \mathbf{1}_{n_x}^\top p_1 \\ \vdots \\ \mathbf{1}_{n_x}^\top p_{N_D} \end{bmatrix} - \begin{bmatrix} \mathbf{1}_{n_x}^\top Qw^{(1)} \\ \vdots \\ \mathbf{1}_{n_x}^T Qw^{(N_D)} \end{bmatrix} + \mathbf{1}_{N_D} \otimes \left(\mathbf{1}_{n_x}^\top Qe_k\right) \tag{16b}$$

Note that the first inequality in (9) can be vectorized as follows:

$$\mathbf{aP} \leq \theta. \tag{17}$$

Here, $\mathbf{a}$ is given by:

$$[\mathbf{a}]_i = \begin{cases} \alpha_i,\ i \in \text{SV} \\ 0,\ \ i \notin \text{SV} \end{cases} \tag{18}$$

whereas $\mathbf{P} = \left[\mathbf{1}_{n_x}^\top p_1 \ \cdots \ \mathbf{1}_{n_x}^\top p_{N_D}\right]^\top$. By multiplying each inequality in equation (16) with $\mathbf{a}$, the inequalities can be rewritten as follows:

$$-\mathbf{a}\left(\mathbf{1}_{N_D} \otimes (\mathbf{1}_{n_x}^\top Q\phi_k)\right) w_\theta \leq \theta + \mathbf{a}\left(\mathbf{I}_{N_D} \otimes (\mathbf{1}_{n_x}^\top Q)\mathbf{w}\right) - \mathbf{a}\left(\mathbf{1}_{N_D} \otimes \left(\mathbf{1}_{n_x}^\top Qe_k\right)\right) \tag{19a}$$

$$\mathbf{a}\left(\mathbf{1}_{N_D} \otimes (\mathbf{1}_{n_x}^\top Q\phi_k)\right) w_\theta \leq \theta - \mathbf{a}\left(\mathbf{I}_{N_D} \otimes (\mathbf{1}_{n_x}^\top Q)\mathbf{w}\right) + \mathbf{a}\left(\mathbf{1}_{N_D} \otimes \left(\mathbf{1}_{n_x}^\top Qe_k\right)\right) \tag{19b}$$

Here, $\mathbf{I}_{N_D} \in \mathbb{R}^{N_D \times N_D}$ and $\mathbf{w} = \left[w_1 \ \cdots \ w_{N_D}\right]^T$ stand for an identity matrix and a vector of historical additive uncertainty data, respectively. Accordingly, the non-falsified parameter set can be defined as follows:

$$\begin{aligned} \Delta_k &= \{w_\theta \mid H_{w,k} w_\theta \leq h_{w,k}\}, \\ H_{w,k} &= \begin{bmatrix} -1 \\ 1 \end{bmatrix} \mathbf{a}\left(\mathbf{1}_{N_D} \otimes (\mathbf{1}_{n_x}^\top Q\phi_k)\right), \\ h_{w,k} &= \begin{bmatrix} \theta + \mathbf{a}\left(\mathbf{I}_{N_D} \otimes (\mathbf{1}_{n_x}^\top Q)\mathbf{w}\right) - \mathbf{a}\left(\mathbf{1}_{N_D} \otimes \left(\mathbf{1}_{n_x}^\top Qe_k\right)\right) \\ \theta - \mathbf{a}\left(\mathbf{I}_{N_D} \otimes (\mathbf{1}_{n_x}^\top Q)\mathbf{w}\right) + \mathbf{a}\left(\mathbf{1}_{N_D} \otimes \left(\mathbf{1}_{n_x}^\top Qe_k\right)\right) \end{bmatrix}. \end{aligned} \tag{20}$$

In order to calculate e_k as defined in (14), the estimate of $(\bar{A}, \bar{B}_d, \bar{B}_u)$ is required. We denote these matrices as $(\hat{A}, \hat{B}_d, \hat{B}_u)$. These matrices can be calculated as follows

$$\left[\hat{A} \ \hat{B}_d \ \hat{B}_u\right] = [A \ B_d \ B_u] - \sum_{i=1}^{4} [A_i \ B_{d,i} \ B_{u,i}]\, \hat{w}_{\theta_i}. \tag{21}$$

The parametric uncertainty estimate is updated according to the following rule (Lorenzen et al., 2019):

$$\begin{aligned} \tilde{w}_{\theta,k+1} &= \hat{w}_{\theta,k} + \gamma\phi_k^\top (x_{k+1} - \hat{A}x_k - \hat{B}_d d_k - \hat{B}_u u_k), \\ \hat{w}_{\theta,k+1} &= \Pi_{\mathcal{W}_{\theta,k}}\left(\tilde{w}_{\theta,k+1}\right). \end{aligned} \tag{22}$$

where $\Pi_{\mathcal{W}_{\theta,k}}$ is a projection operator which is defined as

$$\hat{w}_{\theta,k+1} = \arg\min_{w_\theta \in \mathcal{W}_{\theta,k}} \|w_\theta - \hat{w}_{\theta,k}\|_1 \tag{23}$$

and γ denotes the update step size.

The proposed procedure is summarized in Algorithm 1.

2.3 Uncertain Disturbance Estimation

In addition to parametric uncertainty, an uncertain disturbance is also considered. We assume that the disturbance is unknown but lies in a bounded and convex polytope. Using historical disturbance data $d^{(i)}$ in the data set D, we also apply SVC to estimate the uncertainty set $\mathcal{W}_d$.

2.4 Optimal Control Problem

We implement a robust MPC to regulate the heat supply process to the building. The objective of this controller is

Algorithm 1 SVC-based set membership estimation

Given: Historical data set $D = \left\{w^{(i)},\, d^{(i)},\, u^{(i)}\right\}_{i=0}^{N_D}$

Offline:

1: Choose $\hat{w}_{\theta,0}$ and γ
2: Compute Q
3: Find α, $\mathcal{I}_s$, and $\mathcal{I}_b$ by solving SVC optimization problem (Shang et al., 2017, Section 2.2)

Online: At each time step $k \geq 0$:

1: Compute $\hat{w}_\theta$ using (22)
2: Compute $(\hat{A}, \hat{B})$ using (21)
3: Compute e_k as defined in (14)
4: Compute the non-falsified parameter set as defined in (20)
5: Update parametric uncertainty set estimate using (7)

to minimize the cumulative cost of heating the space over a certain period of time. At the same time, the controller must satisfy the lower and upper temperature limits. The robust optimization problem can be formulated as

$$\min_{\mathbf{u}} \max_{\omega \in \Omega_k} \quad \sum_{l=0}^{H-1} C_{l|k} u_{l|k} \tag{24a}$$

$$\text{s.t.} \quad x_{l+1|k} = \hat{A} x_{l|k} + \hat{B}_u u_{l|k} + \omega_{l|k}, \tag{24b}$$

$$x_{l|k} \in \mathcal{X}_{l|k},\ \forall \omega \in \Omega_k, \tag{24c}$$

$$u_{l|k} \in \mathcal{U}. \tag{24d}$$

Here, ω denotes the total uncertainty that consists of the disturbances and the parametric uncertainty induced additive uncertainty. C and H represent the heating cost and the prediction horizon, respectively. (24c) denotes the state constraint that forces the room temperature to remain within the upper and lower limits. This constraint is given by

$$\mathcal{X}_k = \{F x_k \leq f_k\}\,. \tag{25}$$

(24c) may vary throughout the simulation as the comfort temperature bounds change over different time steps. (24d) ensures that the heat energy input remains within the maximum and minimum values. The input constraint is given by

$$\mathcal{U} = \{G u_k \leq g\}\,. \tag{26}$$

Parametric uncertainty and disturbance sets are used for several purposes. First, the parametric uncertainty set is used to estimate the value of the parametric uncertainty $\hat{w}_\theta$. The parametric uncertainty estimate is also used to estimate the true dynamic matrices $(\bar{A}, \bar{B})$. Another role of parametric uncertainty and disturbance sets is to construct the total uncertainty set that is defined as

$$\Omega_k = \mathcal{W}_k \oplus \hat{B}_d \mathcal{W}_{d,k}. \tag{27}$$

$\mathcal{W}_k$ is an additive uncertainty set induced by parametric uncertainty. This set is defined as

$$\mathcal{W}_k = \big\{w : \, w = \phi(x,u)\left(w_\theta - \hat{w}_{\theta,k}\right), \forall x \in \mathcal{X}, \forall u \in \mathcal{U},\ \forall w_\theta \in \mathcal{W}_{\theta,k}\big\}. \tag{28}$$

The robust MPC algorithm using an SVC-based uncertainty set is described in Algorithm 2.

Algorithm 2 RMPC using SVC-based uncertainty set

Offline:

1: Choose H

Online: At each time step $k \geq 0$:

1: Obtain state x_k
2: Compute Δ_k and $W_{\theta,k}$ using Algorithm 1
3: Compute $\mathcal{W}_k$ and Ω_k using (28) and (27)
4: Solve (24)
5: Apply $u_k = u_{k|k}$

3. NUMERICAL SIMULATION

In this section, we evaluate the performance of the SVC-based parametric uncertainty set estimation technique and RMPC for building thermal control. We compared the SVC-based set estimation technique constructed with a box-shaped set-based non-falsified set. In the subsequent parts of this work, the SVC-based set estimation approach will be denoted as SVC, whereas the box-based approach will be denoted as box. For the RMPC evaluation, we compared an RMPC that uses the SVC-based parametric uncertainty set with another RMPC that uses the box-based parametric uncertainty set. We denote the controller with the SVC-based parametric uncertainty set as RMPC-SVC, whereas the other one is called RMPC-box.

3.1 Simulation Settings

In this simulation, we consider a simple house with building parameters taken from (Kim et al., 2016). Ambient temperature and solar radiation data are perturbed by Gaussian random noise $\mathcal{N}(0, 0.5)$ to emulate forecast uncertainty. The average ambient temperature over the simulation period is 13.65 °C. The dynamical system is discretized with a sampling period $T_s = 15\,\text{min}$. The true lumped parameters are set to $\theta^* := [0.12\,\text{h}^{-1}, 1.77\,\text{h}^{-1}, 0.52\ \ \text{h}^{-1}, 0.85\,^\circ\text{C/kWh}]^\top$. These parameters suffer from constant parametric uncertainty $w_\theta := [0.02, 0.22, -0.09,\ \ 0.14]^\top$. The initial estimate of the parametric uncertainty is $w_{\theta,0} := [0.90, 0.90, 0.90, 0.90]^\top$. The prediction horizon of both types of MPC are $H = 8$ time steps, i.e., 2 h.

Optimization problems for SVC and RMPC were formulated using Matlab® with YALMIP (Löfberg, 2012) and MPT (Herceg et al., 2013). Using YALMIP, we derived robust counterparts of the Min-Max optimization problem. The detailed derivation process follows the mechanism explained in Section 5 of (Löfberg, 2012).Optimization problems are solved using Gurobi®. Set manipulation is done using MPT.

4. RESULTS AND DISCUSSIONS

4.1 Parametric Uncertainty Set

As the parametric uncertainty w_θ lies in a 4-dimensional space, we cannot plot the whole uncertainty set in a single plot. Hence, we projected the uncertainty set into 3 different pairs of dimensions to compare their area. Fig. 1 shows that, using the SVC method, our estimation technique produced a set with a smaller area than the box method.

4.2 Hourly Heat Supply

Fig. 2 shows that all MPCs scheduled a lot of heat supply from the heat source (heating network or space heating

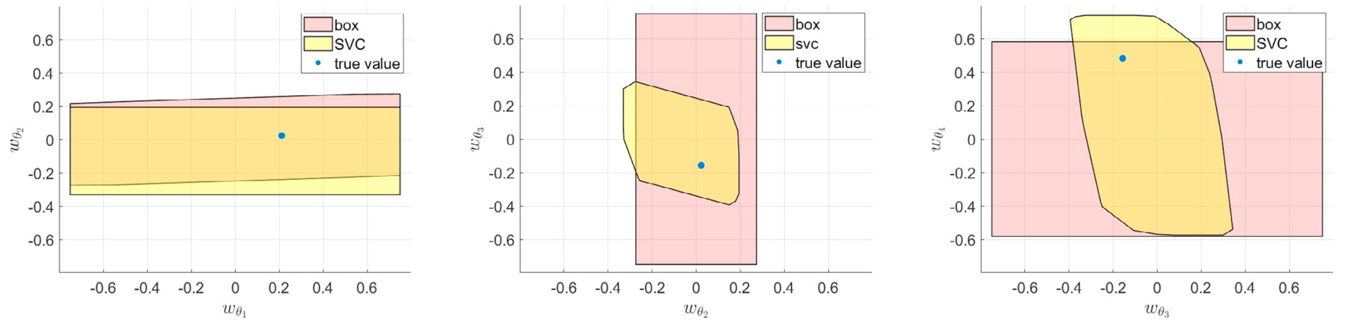

(a) Projection of parametric uncertainty set into the $w_{\theta_1} - w_{\theta_2}$-plane.

(b) Projection of the parametric uncertainty set into the $w_{\theta_2} - w_{\theta_3}$-plane.

(c) Projection of the parametric uncertainty set into the $w_{\theta_3} - w_{\theta_4}$-plane.

Fig. 1. Comparison of the parametric uncertainty set estimated by using box and SVC method. w_{θ_n} axis corresponds to the n-th element of parametric uncertainty vector w_θ.

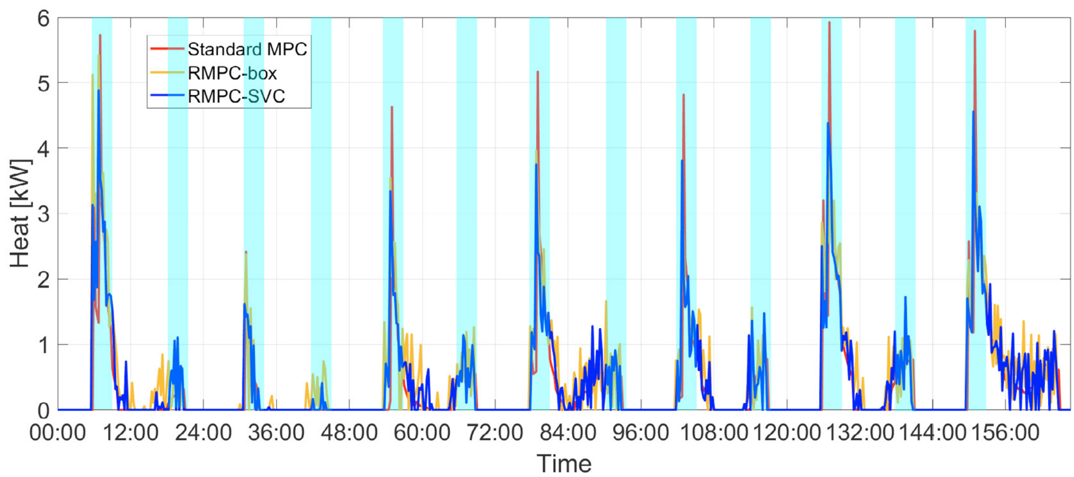

Fig. 2. Comparison of buildings' heat consumption with 3 different MPCs, namely Standard MPC, RMPC-box, and RMPC-SVC. The light blue regions indicate the time periods when the cost of heat generation was low due to the low heat demand. The high heat supply in the morning reflected periods when cost was low, but increases were anticipated due to the increase of the lower limit of room temperature.

.

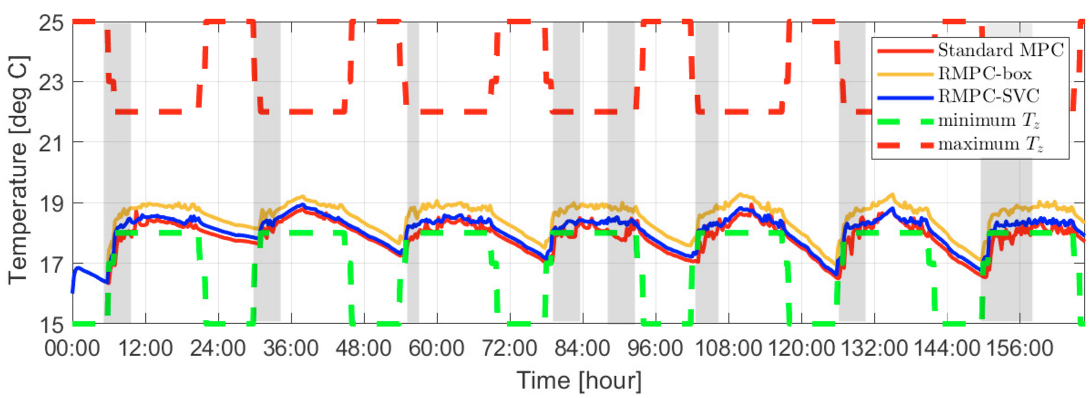

Fig. 3. Comparison of the buildings' temperature evolution trajectory. Each building is controlled by different MPC, namely Standard MPC, RMPC-box, and RMPC-SVC. The gray region indicates the period when the minimum temperature constraints are violated by the standard MPC approach.

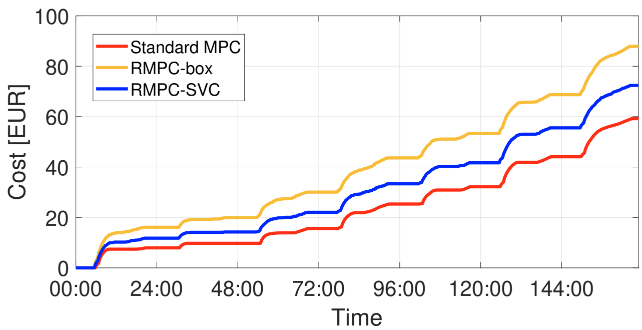

Fig. 4. Comparison of the cumulative energy spending over 7 days under the use of 3 different MPCs, namely Standard MPC, RMPC-box, and RMPC-SVC.

device) when the heat generation cost was low, while avoiding placing orders in other periods. As shown in Fig. 2, the generation cost is low between 06:00 and 09:00, as well as between 18:00 and 21:00. A significant amount of heat was ordered between 06:00 and 09:00 to maintain room temperature above the lower limit between 10:00 and 18:00. Although the generation cost is also cheap between 18:00 and 21:00, not much heat is required, as the minimum temperature in the subsequent periods is considerably low. Therefore, the remaining heat energy in the air and building structure was considered sufficient to maintain room temperature. The controllers' ability to schedule the heat supply under the cost fluctuation by considering the amount of heat available in the air and building structure implies that all MPCs have successfully exploited the thermal inertia of the building.

However, Fig. 2 also shows that between 09:00 and 18:00, the standard MPC and RMPCs work differently. During this period, the standard MPC did not order heat energy. On the other hand, both the RMPC-box and the RMPC-SVC still ordered a small amount of heat. This additional heat supply is used to hedge against undersupply due to building modeling and forecasting errors. The amount of extra heat ordered by the RMPC depends on the size of the estimated uncertainty set. A bigger set leads to higher heat consumption. Accordingly, our RMPC-SVC outperforms the RMPC-box by ordering less additional heat while keeping the room temperature within the comfort bounds.

4.3 Temperature Evolution of the Controlled Building

Fig. 3 shows that a standard MPC failed to satisfy the minimum temperature constraints in numerous time steps without any uncertainty handling measure. Over 668 time steps, the standard MPC violates the lower thermal comfort bound in 134 time steps. However, both RMPCs successfully maintained the controlled building temperature within the thermal comfort bound throughout the simulation.

Even though both RMPCs successfully keep the temperature within the specified bounds, the RMPC-box uses a larger parametric uncertainty set estimate. Since the estimated set is larger, the controller operated conservatively. This means that the controller will steer the temperature farther away from the boundary values than the RMPC-SVC. Although a conservative control policy incurs a lower risk of constraint violation, it severely increases energy bills. Fig. 4 shows that a controlled building with an RMPC box costs approximately €173 after 7 days. This is €52 more expensive than a building managed by a standard MPC. In contrast, RMPC-SVC only increases the bill by €29. Therefore, our new controller can reduce the additional expenditure for uncertainty handling by 44%.

5. CONCLUSION

In this paper, we proposed a parametric uncertainty set construction method based on the SVC set. The resulting set is tighter than typical parametric uncertain sets constructed by a box unfalsified set. Using this tighter uncertainty set, we designed a less conservative robust MPC. A less conservative robust MPC will reduce the cumulative heat cost. Although we apply this robust control strategy for a system whose model is derived using a system identification approach, this framework can also be integrated with other parametric models obtained from different data-driven approaches.

REFERENCES

Ben-Hur, A., Horn, D., Siegelmann, H.T., and Vapnik, V. (2001). Support vector clustering. *Journal of machine learning research*, 2, 125–137.

Herceg, M., Kvasnica, M., Jones, C., and Morari, M. (2013). Multi-Parametric Toolbox 3.0. In *Proc. of the European Control Conference*, 502–510. Zürich, Switzerland. `http://control.ee.ethz.ch/ mpt`.

Kessy, A., Lewin, A., and Strimmer, K. (2018). Optimal whitening and decorrelation. *The American Statistician*, 72(4), 309–314.

Kim, D., Cai, J., Ariyur, K.B., and Braun, J.E. (2016). System identification for building thermal systems under the presence of unmeasured disturbances in closed loop operation: Lumped disturbance modeling approach. *Building and Environment*, 107, 169–180.

Löfberg, J. (2012). Automatic robust convex programming. *Optimization methods and software*, 27(1), 115–129.

Lorenzen, M., Cannon, M., and Allgöwer, F. (2019). Robust MPC with recursive model update. *Automatica*, 103, 461–471.

Milanese, M. and Vicino, A. (1991). Optimal estimation theory for dynamic systems with set membership uncertainty: An overview. *Automatica*, 27(6), 997–1009.

Pothof, I., Vreeken, T., et al. (2023). Data-driven method for optimized supply temperatures in residential buildings. *Energy*, 284.

Reynders, G., Diriken, J., and Saelens, D. (2014). Quality of grey-box models and identified parameters as function of the accuracy of input and observation signals. *Energy and buildings*, 82, 263–274.

Shang, C., Huang, X., and You, F. (2017). Data-driven robust optimization based on kernel learning. *Computers & Chemical Engineering*, 106, 464–479.

Verbeke, S. and Audenaert, A. (2018). Thermal inertia in buildings: A review of impacts across climate and building use. *Renewable and sustainable energy reviews*, 82, 2300–2318.